Monografías de la Real Academia de Ciencias de Zaragoza **31**, 153–174, (2009).

Mathematical problems and solutions in sprinkler irrigation

Enrique Playán[1], Javier Burguete[1], Nery Zapata[1], Raquel Salvador[1], Carlos Bautista-Capetillo[2], José Cavero[1], Antonio Martínez-Cob[1], José Faci[3] and Farida Dechmi[3]

[1] Dept. Soil and Water, Aula Dei Experimental Station, CSIC.
P.O. Box. 202, 50080 Zaragoza, Spain

[2] Maestría en Planeación de Recursos Hidráulicos, Universidad Autónoma de Zacatecas
Av. Ramón López Velarde, 801. Zacatecas, México

[3] Soils and Irrigation Department, CITA, (Agri-Food Research and Technology Center)
Av. Montañana 930, 50059 Zaragoza, Spain.

Abstract

Pressurized irrigation is quickly replacing surface irrigation systems in Spain due to the impulse of irrigation modernization programs. The change in irrigation system is resulting in reduced labour and increased irrigation efficiency and crop yield. The main constraint for sprinkler irrigation is the wind, which severely reduces irrigation uniformity and increases evaporation water losses. Many areas of Spain are characterized by strong winds, and therefore require specific design and management techniques. Such is the case of certain areas of the Ebro Valley depression, where yearly wind averages can exceed 3 m s^{-1}. Mathematical simulation models of sprinkler irrigation are required to predict irrigation performance under different hardware, operation and environmental conditions. Such models are based on ballistic theory, and require the numerical solution of the equations of movement applied to a drop moving in the air from the sprinkler nozzle to the soil surface or the crop canopy. A fourth-order Runge-Kutta method has often been used to solve the governing equations. While ballistic models of sprinkler irrigation were proposed decades ago, the evaluation of their adequacy, their calibration, the optimisation of their execution time, and their application to environment-wise irrigation scheduling remain active fields of research. In this paper, recent advances on these issues are presented. The characterization of sprinkler drops is first presented through a photographic method. In a second step, an algorithm is presented to improve the quality of drop measurements produced with an optical spectropluviometer. In a third phase, a computer model is presented for the ballistic simulation of sprinkler irrigation performance. Next, the model is optimised for computational speed using the technique of Runge-Kutta pairs. Finally, the resulting model is applied to the problem of collective sprinkler irrigation scheduling. The use of mathematical models of sprinkler irrigation in combination with real time meteorological information and remote control of collective irrigation networks will result in relevant water conservation, increased water productivity and the generation of high technology jobs in the agricultural sector. All these benefits are required to ensure the sustainability of irrigated agriculture.

Keywords: Sprinkler irrigation, efficiency, uniformity, ballistic model.

1 Introduction

The central Ebro Valley depression of Spain constitutes an important region for irrigated agriculture, with over 700000 ha of irrigated land. In the central depression, annual precipitation amounts to 250-500 mm, while reference evapotranspiration reaches 800–1100 mm [17]. As a consequence, irrigation is required for agricultural production. Only winter cereals (barley and wheat) can be successfully grown under dryfarming conditions, but complete crop failures happen very often due to water stress. The soils in the valley are shallow and poorly developed. Often, soil salinity is a problem, since the whole valley was an internal sea before the river found its way to the Mediterranean sea. Rivers have modelled the valley landscape, and produced the riparian areas, the hill slopes (glacis) and the plateaus (mesas) where agriculture is currently performed. The large river corridor, extending in a NW-SE direction, channels the prevailing local wind, *Cierzo*.

Irrigation developments have accompanied the development of different cultures in the valley, with the 20th century showing the fastest increase in irrigated area, due to the advent of mechanization and political impulse to government-promoted irrigated areas. Irrigation developments mostly depend on canals transporting water from reservoirs in the Pyrenees Mountains to the fields through distances of up to 100 km. Sprinkler irrigation first appeared in the valley by the 1970s in individual farms profiting from natural pressure or implementing rudimentary pumping stations. In the 1980s the first pressurized collective networks were built in the area.

The processes of irrigation modernization set up by the Government of Spain in cooperation with the regional governments have resulted in a rapid increase of the area devoted to sprinkler and drip irrigation since the beginning of the 21st century [21]. It is foreseen that pressurized irrigation (sprinkler and drip) will soon replace surface irrigation as the most important system in the valley. Today we are in process of rebuilding about half of the surface irrigated area in the valley, switching from surface irrigation to collective sprinkler (and drip) irrigation networks.

The most common sprinkler irrigation systems in the valley are solid sets and pivots.

In solid-sets the field is irrigated from stationary sprinklers emerging from a buried water distribution network. Sprinklers are often arranged in a triangular pattern (Fig. 1), located at around 2 m above de soil surface, and commonly spaced 15–21 m. Pivots are moving irrigation machines performing irrigation in circular areas with radius of about 150–400 m. Water is applied from sprinklers located along the suspended water distribution pipeline at about 4 m above the soil surface [27].

Figure 1.— Aerial view of a sprinkler irrigated area, showing a poor irrigation uniformity resulting from irrigation under strong winds. The photo was extracted from SigPac, a tool for the control of the Common Agricultural Policy elaborated by the Government of Spain (`http://sigpac.mapa.es/fega/visor/`).

In sprinkler irrigation water is applied from the sprinkler nozzle, which produces a jet breaking up in thousands of drops of different diameters. Drops travel for a distance of 2 to 15 m (depending on their diameter) before reaching the soil surface. In the dry, hot and windy conditions of the Ebro Valley, transporting water drops through the air results complicated. The wind modifies the landing place of individual drops, concentrating water application in certain areas. Additionally, wind speed is the most explanatory variable for wind drift and evaporation losses. Despite the use of the best available technology, sprinkler irrigation performance is not always excellent [7].

Irrigation performance is measured using a number of performance indicators [2]. In the case of sprinkler irrigation, the Coefficient of Uniformity (CU, %), proposed by Christiansen [5], is very important. This coefficient expresses numerically the uniformity of water application in the field, so that 100% would be a perfect, unreal uniformity case, in which all parts in the field would receive exactly the same amount of irrigation water. CU can be determined as:

$$CU = \left(1 - \frac{1}{n\overline{x}} \sum_{i=1}^{n} (x_i - \overline{x})\right) 100\%, \tag{1}$$

where:

n is the number of pluviometers evenly distributed in the irrigated area;

x_i is the irrigation water depth received in an individual pluviometer (mm); and

$\overline{x}$ is the average irrigation water depth received in the pluviometers (mm).

Another indicator commonly used in sprinkler irrigation is the Potential Application Efficiency of the Low Quarter ($PAElq$, %), as defined by Merriam and Keller [18] and revised by Burt et al. [2]. $PAElq$ applies to an irrigation event, and can be expressed as:

$$PAElq = \frac{\text{average depth of irrigation water contributing to the target}}{\text{average depth of irrigation water applied such that } d_{lq} = \text{target}} 100\%. \tag{2}$$

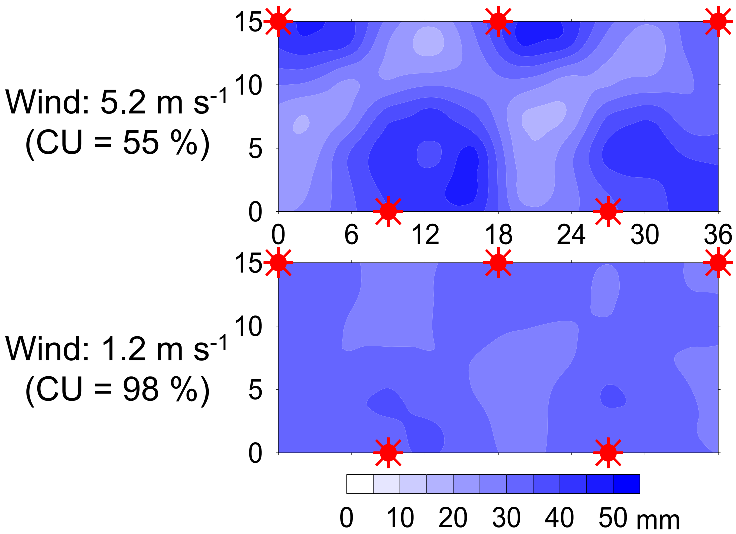

Figure 2.— Maps of water distribution in a triangular 18 x 15 m sprinkler irrigation solid-set operating at two wind speeds

The problems resulting from sprinkler irrigation under strong wind in the Ebro Valley are evident in Fig. 1 extracted from SigPac, a tool for the control of the Common Agricultural Policy elaborated by the Government of Spain (`http://sigpac.mapa.es/fega/visor/`).

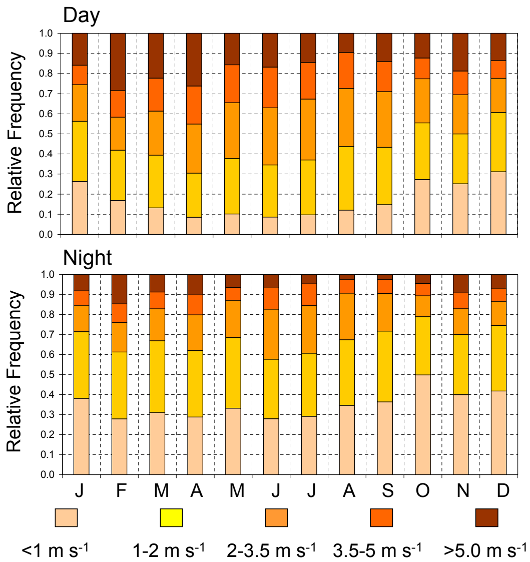

Figure 3.— Analysis of wind intensity in Zaragoza during day and night time. Figures present the relative frequency of wind classes in different months. Data were obtained at the CITA experimental farm automated station in the period 1995-2002. Daytime was assumed as 7:00-19:00 GMT

The aerial photograph shows the results of sprinkler irrigation, with water accumulating in certain areas of the field and being applied in very small amounts in other areas. Consequently, crop growth is intense in certain areas, while in other areas water stress decreases crop growth and results in yield losses. This problem is further illustrated by Fig. 2 [6], developed under experimental conditions. In the Figure, maps of irrigation water depth isolines corresponding to two irrigation events differing in wind speed are compared. In the high wind speed irrigation event (5.2 m s^{-1}), water accumulated in parts of the field downstream from the sprinkler, and *CU* only reached 55%. In the low wind speed irrigation event (1.2 m s^{-1}), water application was more uniform and *CU* reached 98%. In order to minimize these problems, farmers can adapt the design of the irrigation system (narrow sprinkler spacing, sprinklers located at lower height from the soil surface, avoid high operating pressures?). They can also adapt irrigation management by selecting the irrigation time, looking for periods of low wind.

Fig. 3 shows that even under the prevailing windy conditions of the Ebro Valley low wind speed periods can be effectively selected. The Figure presents an analysis of monthly wind intensity in Zaragoza separating day and night time. Subfigures present the relative frequency of wind classes in different months. Daytime was assumed to last from 7:00 to 19:00 GMT (Greenwich Mean Time). The two low-wind classes (0–2 m s^{-1}) represent the prime time for irrigation, according to the wind speed thresholds proposed by Faci and Bercero [10] for adequate sprinkler irrigation. These two wind classes represent 40–50% of the day time and about 70% of the night time in Zaragoza. Night time irrigation thus

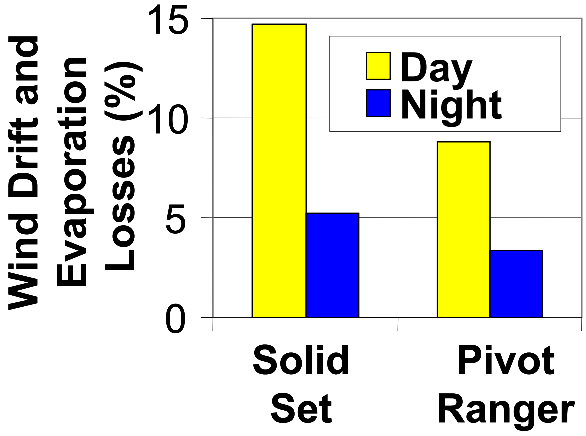

Figure 4.— Average wind drift and evaporation losses resulting from solid-set and pivot (or ranger, a linear-move machine) irrigation, operating during day and night conditions

represents a clear advantage to obtain high irrigation uniformity. Night irrigation can be easily performed by means of automated irrigation programmers.

The effect of irrigation technology and day/night irrigation on wind drift and evaporation losses is illustrated in Fig. 4, which presents the percentage of water emitted by the sprinkler and not reaching the soil surface under different conditions [22]. Night time irrigation reduces these water losses to roughly one-third as compared to day time irrigation, while pivot irrigation and linear move irrigation systems (ranger) reduce losses to about two-thirds, when compared to solid-set sprinkler irrigation. Once an irrigation system is in place, farmers can only modify the time of irrigation to maximize uniformity and to minimize water losses. The selection of appropriate irrigation time is hampered by the generalised use of irrigation programmers executing rigid, wind-insensitive irrigation orders.

This paper presents the problematic of sprinkler irrigation from a mathematical point of view, and provides mathematical solutions to these problems. The goal is to illustrate the relationship between mathematics and agricultural water management in the specific field of sprinkler irrigation. The addressed problems include:

- characterization of sprinkler drops using photography;
- a disdrometer for drop characterization: minimizing measurement errors;
- a ballistic model of sprinkler irrigation based on drop diameter distribution;
- optimizing the ballistic model for computational speed: Runge-Kutta pairs; and
- collective irrigation scheduling: optimising daily irrigation operation.

2 Characterization of sprinkler drops using photography

Different methodologies have been reported in the literature to manually determine drop diameters resulting from precipitation, sprinkler irrigation or pesticide application. Montero et al. [20] discussed a series of manual methods based on impression, photography, immersion in viscous fluids and impact on a layer of flour.

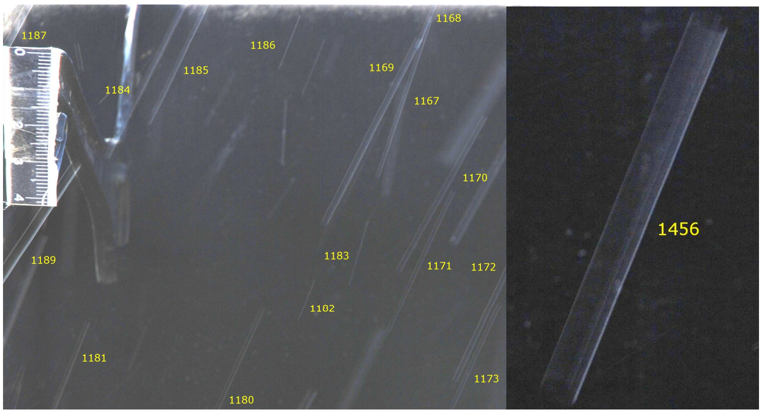

Figure 5.— Photograph of water drops resulting from outdoor sprinkler irrigation. The camera was set at a shutter speed of 1/100 s. Drops in focus were numbered (left) and prepared for the measurement of drop diameter, drop angle and length (right)

This section describes a new, reliable, methodology aiming at describing the diameter and velocity of sprinkler irrigation generated drops. A VYR35 impact sprinkler (VYRSA, Burgos, Spain) was used in this experiment. This sprinkler model is commonly used in solid-set systems in Spain. The sprinkler was equipped with a 4.8 mm nozzle (including a straightening vane). An isolated sprinkler was installed at an elevation of 2.15 m and operated at a nozzle pressure of 200 kPa. A digital photographic camera (Nikon D80) equipped with a 18–70 mm lens was installed at an elevation of 0.80 m, and adjusted to a shutter speed of 100 (1/100 s) and F11. A black cloth screen was installed at a distance of 1.0 m. The screen had a millimetric ruler located at a distance of 0.25 m towards the camera. The camera was focused at the ruler. Photo quality "L" (3872×2592 pixels) was selected because this was the highest available image resolution in JPEG format, and the picture taking speed was acceptable (9 photos in the first 3.1 seconds, one photo each 1.13 seconds later on). The combination of photo quality, zoom regulation and distance to the target resulted in a linear density of 14–15 pixels mm^{-1}. More details on the experiments and its results can be found in Salvador et al. [25]. The camera was located at different distances from the sprinkler and operated on continuous shooting mode (2.9 photos s^{-1}) whenever the sprinkler water reached it.

After digital treatment of the resulting images, drops appeared as transparent cylinders (Fig. 5). The Figure presents a set of drops and the ruler (left), and an individual drop (right). Drop diameter, length and angle were individually measured. Drop velocity was derived from drop length and shutter speed. For each distance to the sprinkler, a set of drop diameters and velocities was obtained. Fig. 6 presents histograms of these two variables, which show very important changes along the distance irrigated by a sprinkler. Proximal drops have diameters below 1 mm (with a few exceptions), and velocities lower than 3 m s^{-1}. Distal drops show very different features, with well-graded diameters with modal values in the 3–4 mm range and most drops in the velocity range of 5–6 m s^{-1}.

These data permit to gain knowledge on drop diameter and velocity distributions measured individually in a series of experiments. The method is very time consuming, but permits individual drop characterization, very well suited for comparison with automated drop characterization methods, such as the disdrometer.

3 A disdrometer for drop characterization: minimizing measurement errors

Manual methods of drop characterization have been largely replaced by computer driven optical devices, owing to experimental speed and repeatability. Among them, optical methods using laser equipment [13] and optical disdrometer methods [20].

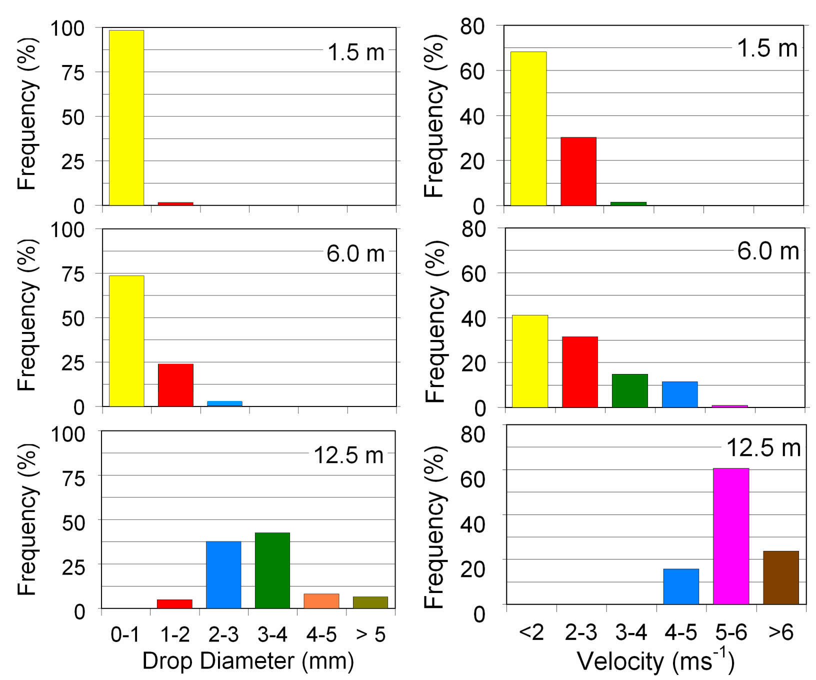

Figure 6.— Histograms of water drop diameter and velocity at different distances to the sprinkler (1.5, 6.0 and 12.5 m)

Optical disdrometers measure the attenuation of an infrared beam when water drops pass across it. The beam section is circular in shape and centimetric in diameter. As a

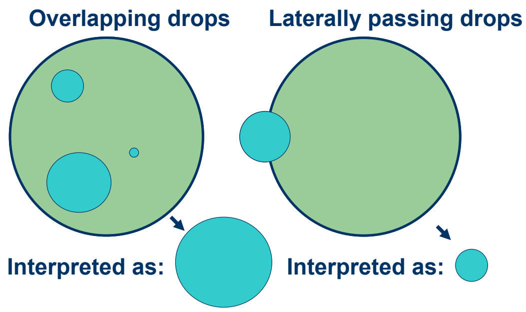

Figure 7.— Sources of error in the interpretation of disdrometer signal: overlapping drops and laterally passing drops

drop passes between the beam emitter and the detector, a decrease in electric potential is measured at the detector which is proportional to the drop shadow [20]. The technique permits to measure drop size and time of passage as each drop passes through a stationary detector. These variables are very relevant to validate sprinkler irrigation models. However, two experimental problems affect the quality of these measurements [20]: first, several drops can overlap as they reach the disdrometer. In these circumstances the device will detect only one drop, with larger-than-real size and time of passage; and second, drops can pass through a side of the detector, so that only part of the drop attenuates the luminous flow. As a consequence, the drop size and time of passage will be shorter-than-real.

These two problems are illustrated in Fig. 7, and can happen in a variety of cases, resulting in anomalous detections. As mentioned above, drops of a given diameter reach the disdrometer at statistically similar velocities (Fig. 6). Consequently, a statistical treatment of time of passage should suffice to eliminate a relevant part of the erroneous measurements. This principle constitutes the basis for a statistical method for the treatment of disdrometer data reported in this section [1].

Let uss assume a spherical drop with radius r passing across a circular detector with radius R with velocity v in a 2D coordinate system XZ (Fig. 8). The average time of drop passage can be determined as:

$$\overline{T} = \frac{\displaystyle\int_{-R-r}^{R+r} \frac{2\sqrt{(R+r)^2 - x^2}}{v}\,\mathrm{d}x}{\displaystyle\int_{-R-r}^{R+r} \mathrm{d}x} = \frac{\pi}{2}\frac{R+r}{v}. \tag{3}$$

Two criteria can be established for drop i (characterized by detected radius r_i and time of passage t_i) in order to detect the abovementioned sources of error. Due to the statistical nature of drop data, criteria are defined using a tolerance τ. The first criterion addresses overlapping drops, and can be formulated as:

$$t_i > (1+\tau)\frac{4}{\pi}\overline{T}. \tag{4}$$

The second criterion addresses laterally passing drops, and can be formulated as:

$$t_i < (1+\tau)\frac{8}{\pi}\frac{\sqrt{Rr_i}}{R+r_i}\overline{T}. \tag{5}$$

These criteria were formulated in an application sequentially analysing the set of drops resulting from a disdrometer analysis of sprinkler drops. Drops failing to meet the reported criteria are rejected and excluded from the set, since they are likely to result from the reported errors in disdrometer functioning. The application iteratively determines the optimum value of t based on thresholds of percentage of rejected drops.

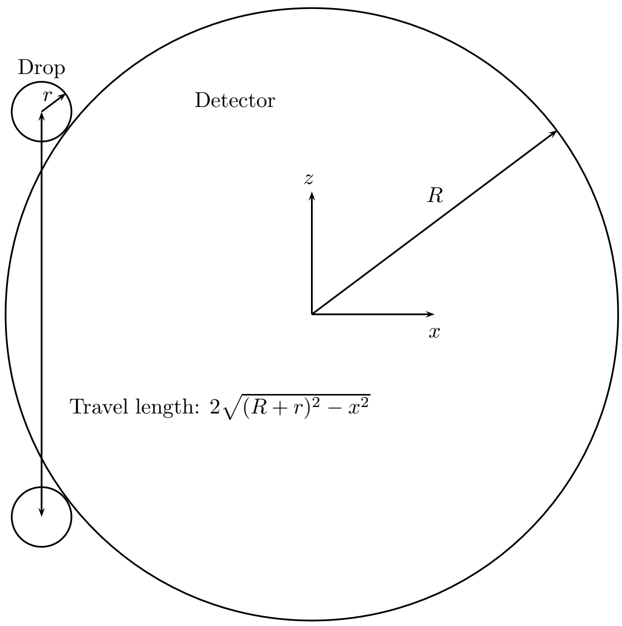

Figure 8.— Diagram of a drop with radius r passing vertically across a circular detector with radius R in a 2D coordinate system XZ

A numerical experiment was devised to assess the improvements derived from the proposed method [1]. The experiment is based on the pseudo-random generation of a set of drop diameters and times of passage. This data followed a triangular diameter frequency law, with diameters between 1 and 8 mm, and the modal value at 4 mm. In the test, the passage of a set of 200000 synthetic drops was geometrically simulated and the simulated drop detected diameters were compared to the real drop diameters. Fig. 9 presents the experimental results. The detected set of diameters (a,c,e) showed relevant deviations from the input triangular histogram. In this particular case, errors resulted from an underestimation of the frequency of small drops and the overestimation of large drops. The proposed method of drop rejection resulted in much more triangular drop diameter histograms, which still reveal some differences with the original set of

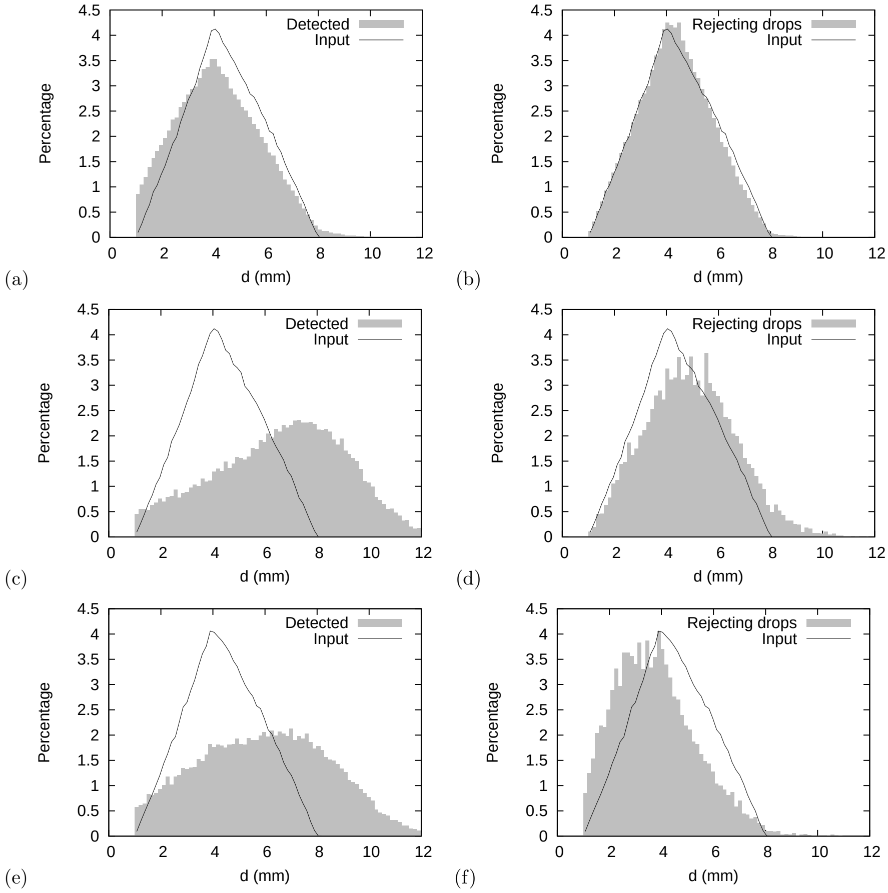

Figure 9.— Results of the experimental test of erroneous drop rejection. The input drop diameter histogram is compared to the histograms of detected and modified (through the drop rejection method) drop diameter

drop diameter data. The method proved to be an important tool in the valorisation of disdrometer data as applied to the high drop densities resulting from sprinkler irrigation.

4 A ballistic model of sprinkler irrigation based on drop diameter distribution

Fukui et al. [11] presented the basic equations and procedures for ballistic simulation of sprinkler irrigation. Recently, Carrin et al. [4] and Montero et al. [19] presented the SIRIAS software, which further developed ballistic theory and presented it in a user-friendly environment.

Dechmi et al. [8, 9] and Playán et al. [23] presented Ador-sprinkler, a ballistic sprinkler irrigation model which was used in combination with a crop model. They showed that the sprinkler irrigation model could successfully reproduce the water distribution pattern observed in the field ($R^2 = 0.871$). Moreover, a crop simulation model using the simulated water distribution pattern as input resulted in simulated values of yield reduction which could explain the field observed values ($R^2 = 0.378$). The main characteristics of the ballistic model presented in this work are discussed in the following paragraphs.

A sprinkler is simulated as a device emitting drops of different diameters. It is assumed that drops are formed at the sprinkler nozzle, and travel independently until reaching the soil surface (or the crop canopy). Ballistic theory is used to determine the trajectory of each drop diameter subjected to an initial velocity vector and a wind vector (**U**, parallel to the ground surface). The action of gravity (acting in the vertical direction) and the resistance force (opposite to the drop trajectory) complete the analysis of forces acting on the water drop. The drop velocity with respect to the ground (**W**) is equal to the velocity of the drop in the air (**V**) plus the wind vector (**U**).

According to Fukui et al. [11], the three directional components of the movement of each drop can be expressed as:

$$A_x = \frac{d^2x}{dt^2} = -\frac{3\rho_a C}{4\rho_w D} V\left(W_x - U_x\right), \qquad A_y = \frac{d^2y}{dt^2} = -\frac{3\rho_a C}{4\rho_w D} V\left(W_y - U_y\right),$$

$$A_z = \frac{d^2z}{dt^2} = -\frac{3\rho_a C}{4\rho_w D} V W_z - g, \tag{6}$$

where x, y and z are coordinates referring to the ground (with origin at the sprinkler nozzle), t is the time, ρ_a is the air density, ρ_w is the water density, **A** is the acceleration of the drop in the air, D is the drop diameter, and C is a drag coefficient, which can be expressed as a function of the Reynolds number of a spherical drop and the kinematic viscosity of the air [26].

Equations (6) are solved in the model using a fourth-order Runge-Kutta numerical integration technique. The main result of each drop trajectory solution is constituted by the x and y coordinates of the drop when the z coordinate equals 0 (the soil surface), or the crop canopy elevation, or the catch can elevation. In order to reproduce the water application pattern resulting from an isolated sprinkler, these equations must be solved for a number of horizontal sprinkler angles (due to the sprinkler rotation) and for a number of drop diameters. The model typically uses 180 horizontal sprinkler angles and 180 drop diameters, evenly distributed between 0.0002 and 0.007 m. When the landing coordinates of each drop diameter are combined with the fraction of the sprinkler discharge which is emitted in this drop diameter, the water application pattern can be simulated.

In order to characterize the frequency of the drop diameter classes, the abovementioned photographic method or the statistically corrected disdrometer procedure can be used. An alternative procedure consists on using the ballistic model to simulate the landing distance of different drop diameters resulting from a given sprinkler model, nozzle elevation and operating pressure in the absence of wind. The percentage of the irrigation water collected at each landing distance can be used to estimate the percentage of the irrigation water emitted in drops of a given diameter.

As previously discussed, a significant part of the water emitted by a sprinkler does not reach the soil surface, because it either evaporates or drifts away. This water constitutes the Wind Drift and Evaporation Losses ($WDEL$), which are expressed as a percentage of the emitted discharge. Salvador [24] and Playán et al. [22] presented a number of empirical equations aiming at the prediction of $WDEL$ using meteorological variables.

Seginer et al. [26] proposed a correction for the drag coefficient C to reproduce the deformation of the circular water application area produced by the wind. Tarjuelo et al. [28] further refined these corrections, arriving to the following expression:

$$C' = C(1 + K_1 \sin\beta - K_2 \cos\alpha), \tag{7}$$

where α is the angle formed by vectors $\mathbf{V}$ and $\mathbf{U}$, β is the angle formed by the vectors $\mathbf{V}$ and $\mathbf{W}$, and K_1 and K_2 are empirical parameters.

In order to simulate solid-set irrigation, the model overlaps a number of sprinklers located at coordinates reproducing a given sprinkler spacing. For this purpose, 16 sprinklers are used in rectangular layouts and 18 in triangular layouts. The central sprinkler spacing is divided into a number of rectangular cells, with a default 5×5 arrangement. The resulting number of cells (25 in this case) must be equal to the number of catch cans used in the field experiments.

Each drop landing in this central sprinkler spacing is assigned to one of the cells, according to the landing coordinates. The simulated water application in each cell is computed from the number of drops of each diameter and the percent of the sprinkler discharge corresponding to that particular drop diameter. Water application in the cells is further used to determine the simulated coefficient of uniformity.

In summary, the input required to run the described model includes:

- Sprinkler hardware
  - Sprinkler model
  - Nozzle diameter
  - Sprinkler height above the soil surface
  - Sprinkler spacing and arrangement (triangular vs. rectangular)
  - Sprinkler line orientation (azimuth)
- Sprinkler operating pressure and irrigation time
- Drop characterization
  - Frequency of different drop diameters, obtained by:
    * Experimentation, or

* Inverse modelling, adjusting to observed water application

  – Wind empirical parameters

• Meteorological conditions, mainly wind speed and direction.

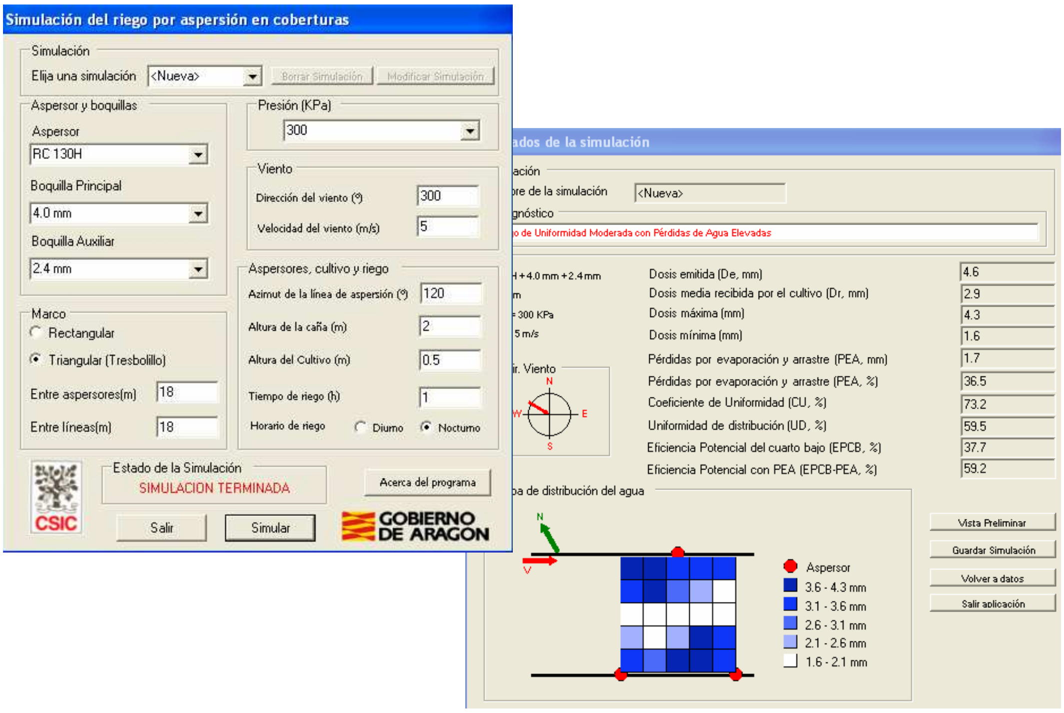

Figure 10.— Input (top) and output (bottom) dialog boxes of the Ador-sprinkler irrigation simulation model

Fig. 10 presents printouts of the input and output windows of the described model interface (in Spanish). The input window contains all the abovementioned parameters. The output window presents a map of water application (in the 25 cells of the sprinkler spacing), along with a series of irrigation performance parameters and a text diagnosis of irrigation performance.

5 Optimizing the ballistic model for computational speed: Runge-Kutta pairs

The time required to run a typical Ador-sprinkler simulation in a 1.73 GHz Pentium processor was about 50 s. We judged this simulation time excessive for use in applications requiring successive simulations, and therefore the model was optimized for execution time. The procedure was based on the optimization of the Runge-Kutta time step using two criteria: numerical stability and error control, and was presented by Zapata et al. [29].

First, a coordinate system was proposed that moves with wind speed. Drag forces can slow down drop movement until it stops. However, the drop can not move backwards in this coordinate system. This physical and mathematical principle can not be numerically violated, and thus establishes a condition on the time step. In the proposed system of coordinates drop movement equations can be written as:

$$\ddot{\mathbf{r}}_w = -\delta \left|\dot{\mathbf{r}}_w\right| \dot{\mathbf{r}}_w + \mathbf{g}, \tag{8}$$

where $\mathbf{r}_w$ is the drop position vector in the cited system of coordinates, $\delta = \frac{3\rho_a C}{4\rho_w D}$ represents aerodynamic drag, and $\mathbf{g}$ the gravitational field. Solving (8) with a first order Runge-Kutta, and using a time step Δt:

$$\dot{\mathbf{r}}_w(t+\Delta t) = \dot{\mathbf{r}}_w(t) + \Delta t \ddot{\mathbf{r}}_w(t) = \dot{\mathbf{r}}_w(t) + \Delta t \left[-\delta \left|\dot{\mathbf{r}}_w\right| \dot{\mathbf{r}}_w + \mathbf{g}\right], \tag{9}$$

which in the horizontal coordinates results in:

$$V_x(t+\Delta t) = V_x(t) - \Delta t \delta(t) V(t) V_x(t), \qquad V_y(t+\Delta t) = V_y(t) - \Delta t \delta(t) V(t) V_y(t). \tag{10}$$

The no backwards movement condition can be formulated as:

$$0 \le \frac{V_x(t+\Delta t)}{V_x(t)} = 1 - \Delta t \delta(t) V(t), \qquad 0 \le \frac{V_y(t+\Delta t)}{V_y(t)} = 1 - \Delta t \delta(t) V(t), \tag{11}$$

resulting in the following condition for the time step:

$$\Delta t \le \frac{1}{\delta V}. \tag{12}$$

Error estimation is required in order to build an efficient solver respecting a certain tolerance [12]. However, a Runge-Kutta method does not estimate error at each time step. Runge-Kutta pairs ([3], and references therein) were designed to estimate error through the use of two different-order Runge-Kutta methods with similar time steps. Given a maximum tolerance (in absolute value) for the final solution (E_{max}) over the total time (t_f) the numerical error will be within the tolerance if in each time step Δt_i the local error e_i (also in absolute value) satisfies:

$$e_i \le \frac{\Delta t_i E_{max}}{t_f}. \tag{13}$$

If the condition is not satisfied, the time step will be reduced to one half. If the Runge-Kutta pairs are used to estimate an error of order n:

$$e_i = \alpha \left(\Delta t_i\right)^n, \tag{14}$$

with α constant and independent of Δt_i. The use of a time step Δt_j leads to:

$$e_j = \alpha \left(\Delta t_j\right)^n = e_i \left(\frac{\Delta t_j}{\Delta t_i}\right)^n. \tag{15}$$

The number of time steps of size Δt_j needed to complete the solution is $t_f/\Delta t_j$. Therefore, in order to maintain the final error within the tolerance:

$$E_{max} = \frac{t_f e_j}{\Delta t_j} = \frac{t_f e_i \left(\Delta t_j\right)^{n-1}}{\left(\Delta t_i\right)^n} \Rightarrow \quad \Delta t_j = \left[\frac{E_{max} \left(\Delta t_i\right)^n}{t_f e_i}\right]^{\frac{1}{n-1}}. \tag{16}$$

This equation can be used to estimate the next time step size:

$$\Delta t_{i+1} = \min \left\{\gamma \Delta t_i,\ \beta \left[\frac{E_{max} \left(\Delta t_i\right)^n}{t_f e_i}\right]^{\frac{1}{n-1}},\ \frac{1}{\delta_i V_i}\right\}, \tag{17}$$

where a parameter $\beta \in (0, 1]$ is introduced as a conservative criterion to ensure that (14) holds and a factor γ is introduced to have the next time step be similar to the previous one.

A numerical case study was devised to demonstrate the improvements in execution time and to test β and γ. The simplified, windless droplet dynamics equations presented by Lorenzini [16], along with their analytical solution, were used in this numerical experiment. A set of 20000 drops with random diameters distributed in the range 0.2–7.0 mm were launched from an elevation of 2.3 m with an initial speed of 24 m s^{-1}, a vertical angle of 25°, and facing a wind with random speed in the interval 0–16 m s^{-1} and random direction in the interval 0–360°. The results were evaluated in terms of the Root Mean Square Error ($RMSE$) in drop landing distance (m) between numerical and analytical solutions *vs.* the number of function calls. Results were produced for different Runge-Kutta pairs, with the RK2-3 pair (orders 2 and 3) resulting the most efficient for virtually all the range in tolerance. A tolerance of 1 m produced —after a bit more than a million function calls— solutions with a maximum error of 0.2 m and an $RMSE$ of 0.05 m. Introducing this technique resulted in increased computational efficiency and accuracy, but also in a control of the numerical error. Experimentation on the values of β and γ for the 2-3 Runge-Kutta pair revealed that values of 1.0 and 1.6, respectively, result in efficient and robust simulations.

When applied to a typical sprinkler irrigation simulation, the optimized model required a computational time of 5 s, resulting in a 90% reduction with respect to the base case. The increase in computational time results very important for real-time model applications oriented to irrigation management, such as the application presented in the following section.

6 Collective irrigation scheduling: optimising daily irrigation operation

The irrigation modernization projects described at the beginning of this work include a public long-term financing scheme. As a consequence, farmers have to accept a number of conditions imposed by public water and agricultural agencies. Among them is the need to install a remote control system that permits to open and close all network valves from the district office. The combination of remote control hardware and real-time meteorology and crop water requirements information via a district-wide irrigation scheduling software could result in an entire automation of the irrigation district operation. Such a system could dramatically reduce the farmers' labour input and at the same time conserve water, ensure high yields and optimize water productivity by timely providing crop water requirements, avoiding unsuitable periods for irrigation (i.e., high winds), and adjusting the irrigation level to the economic conditions of the crop. In this section we present a simulation exercise based on real data from the Ebro basin in Spain which is aimed at providing insight on the possibilities for collective irrigation controllers and on their benefits to agricultural water management. More details on this research can be found in Zapata et al. [29].

A representative portion of the Montesnegros Irrigation District (MID, located in Bujaraloz, Zaragoza, Spain) was selected for model development and application. The simulation area is located in the south-west of the district, is characterized by a flat topography and has a total area of 113 ha. The area is divided in 28 catastral plots owned by 21 farmers. A total of 15 hydrants provide water supply to the on-farm solid-set systems. The average size of the plot is 4.35 ha, with a minimum size of 0.6 ha and a maximum of 25 ha. In 2004 the two main crops in the simulated area were corn and alfalfa, with respective acreage of 63% and 21% of the total area, respectively. The rest of the area (16%) was occupied by winter cereals. Seasonal water used in 2004 in the simulation area (9387 m^3 ha^{-1}) was similar to the MID average for corn, but in the case of alfalfa it was clearly higher (12270 m^3 ha^{-1}).

The Ador-Simulation software has been designed to simulate centralized irrigation control in a solid-set irrigated district. The model is composed by four modules that interchange input and output data to decide the irrigation timing of each plot and to evaluate the effects of irrigation scheduling on crop yield. The four modules are: Ador-Sprinkler, Ador-Crop, Ador-Network and Ador-Decision. The joint operation of the first two modules was presented by Dechmi et al. [8]. Lecina and Playán [14, 15] presented a similar model for surface irrigated districts, including modules for the irrigation network (irrigation canals and reservoirs) and for irrigation decision making.

The long term objective of this research is to automatically make irrigation decisions along the season and to apply them to the irrigated plots via a remote control system. In the applications reported in this paper the application has been evaluated via the crop model. Therefore, simulation was not performed in real time but at the machine speed. Meteorology was introduced in the model through two sources of data: average daily data for crop modelling, and semihourly data for irrigation modelling and decision making.

Ador-Decision is the core module of the proposed model, since this is where irrigation decisions are made taking into account the crop status, water availability (whether a shared hydrant is currently occupied by other users or not) and the projected irrigation performance. Two indicators are used in this module to decide on irrigation: $PAElq$ and ES. The first indicator is $PAElq$ (%), as previously defined. The second indicator, ES (Equivalent Stress, days), is agronomic in nature and indicates the number of days that a plot has been requiring an irrigation to alleviate its water stress. The ES parameter can be determined every day using the built-in crop simulation module. In a model run the user establishes the thresholds for both indicators: a minimum $PAElq$ and a maximum ES. If in a given plot the value of ES is higher than the threshold, irrigation can proceed even it $PAElq$ is lower than the threshold.

Two management strategies were designed for simulation purposes and implemented in Ador-simulation:

Manual. This strategy reproduces a situation in which farmers strictly follow the indications of an irrigation advisory service. They receive crop water requirements based on the previous week and program their plot irrigation controllers every week. Common irrigation scheduling practices in the study area are far from this ideal situation, since farmers do not update their programmers so often.

Central. This strategy is based on real-time model execution and on broadcasting hydrant open/close orders throughout the remote control system. Irrigation starts in a given plot if 1) more than 50% the plot is under water stress; 2) the hydrant is idle; 3) the farmer can irrigate in that given day (this condition applies only to shared hydrants), and 4) requirements on $PAElq$ and ES are met.

The results of these two management strategies were compared to the observed water use in the simulation area using 2005 data. Fig. 11 presents the results in terms of average and standard deviation (among all simulated plots) seasonal water use per crop (alfalfa and corn) as observed and simulated with both strategies. The results show that there is a large margin for water conservation in current crop water use. Adoption of the Manual strategy would require weekly updates of the current irrigation programmers by the farmers. Implementing this strategy would not be easy at the current balance between labour cost, water cost and crop profit. The manual strategy does lead to significant water conservation, particularly in the case of alfalfa. Yield increases could be expected from improved irrigation scheduling. Adopting the Central scheduling strategy would lead to the seasonal conservation of more than 2000 m^3 ha^{-1}, a very sizable amount of water. Development of software applications like the one described in this work, promoting the due maintenance and reliability of remote control systems and fostering farmers' adoption of centralized irrigation will be required in order to conserve this amount of water on a regional basis.

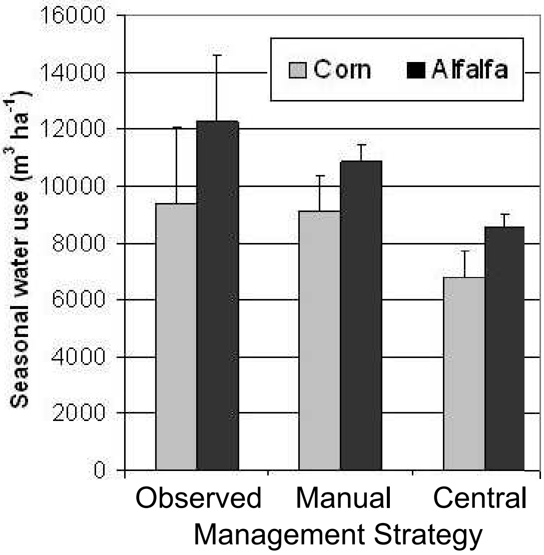

Figure 11.— Irrigation seasonal water use for corn and alfalfa in the conditions of Bujaraloz (Zaragoza, Spain) as observed and simulated with the manual and central strategies

7 Conclusions

- Mathematical and numerical modelling has permitted to develop tools to obtain better design and management tools for sprinkler irrigation systems.
- Some applications of these tools have already been found in the characterization of sprinkler irrigation material and in the design of on-farm irrigation systems.
- A number of relevant applications await development and adoption by farmers. Irrigation is characterized by the need to govern sparse pieces of equipment using meteorological, water resources and crop data which are available in the Internet. The deployment of collective irrigation schedulers will require further development of simulation models and complex decision making routines.
- When farmers are left the role of supervising fully automated collective irrigation controllers, the role of applied mathematics in irrigation water management will still be more important than today.

Acknowledgements

This research was funded by the Plan Nacional de I+D+i of the Government of Spain, through grants AGL2004-06675-C03 and AGL2007-66716-C03; and by grants P028/2000 and PIP090/2005 of the CONSI+D of the Government of Aragón, Spain. Carlos Bautista-Capetillo received a scholarship from the Agencia Española de Cooperación Internacional (AECI).

References

[1] J. Burguete, E. Playán, J. Montero, N. Zapata, Improving drop size and velocity estimates of an optical disdrometer: implications for sprinkler irrigation simulation, Transactions of the ASABE 50 (6) (2007) 2103–2116.

[2] C. M. Burt, A. J. Clemmens, T. S. Strelkoff, K. H. Solomon, R. D. Bliesner, L. A. Hardy, T. A. Howell, D. E. Eisenhauer, Irrigation performance measures: efficiency and uniformity, ASCE Journal of the Irrigation and Drainage Division 123 (6) (1997) 423–442.

[3] J. C. Butcher, The numerical analysis of ordinary differential equations, John Wiley & Sons Inc., New York, 1987.

[4] P. Carrión, J. M. Tarjuelo, J. Montero, SIRIAS: a simulation model for sprinkler irrigation I: description of model, Irrigation Science 20 (2001) 73–84.

[5] J. E. Christiansen, Irrigation by sprinkling, Agric. Exp. Stn. Bull. 670. Univ. of California, Berkeley.

[6] F. Dechmi, Water management in sprinkler irrigation systems in the Ebro Valley: current situation and scenario analysis, Ph.D. thesis, Universitat de Lleida, Lleida, Spain (2003).

[7] F. Dechmi, E. Playán, J. Cavero, J. M. Faci, A. Martínez-Cob, Wind effects on solid set sprinkler irrigation depth and corn yield, Irrigation Science 22 (2) (2003) 67–77.

[8] F. Dechmi, E. Playán, J. Cavero, A. Martínez-Cob, J. M. Faci, A coupled crop and solid set sprinkler simulation model I: model development, ASCE Journal of Irrigation and Drainage Engineering 130 (6) (2004) 499–510.

[9] F. Dechmi, E. Playán, J. Cavero, A. Martínez-Cob, J. M. Faci, A coupled crop and solid set sprinkler simulation model II: model application, ASCE Journal of Irrigation and Drainage Engineering 130 (6) (2004) 511–519.

[10] J. M. Faci, A. Bercero, Efecto del viento en la uniformidad y en las pérdidas por evaporación y arrastre en el riego por aspersión, Investigación Agraria: producción y protección vegetal 6 (2) (1991) 171–182.

[11] Y. Fukui, K. Nakanishi, S. Okamura, Computer evaluation of sprinkler irrigation uniformity, Irrigation Science 2 (1980) 23–32.

[12] T. E. Hull, W. H. Enright, B. M. Fellen, A. E. Sedgwick, Comparing numerical methods for ordinary differential equations, SIAM Journal on Numerical Analysis 9 (4) (1972) 603–637.

[13] D. C. Kincaid, Spraydrop kinetic energy from irrigation sprinklers, Transactions of the ASAE 39 (1996) 847–853.

[14] S. Lecina, E. Playán, A model for the simulation of water flows in irrigation districts I: description, ASCE Journal of Irrigation and Drainage Engineering 132 (4) (2006) 310–321.

[15] S. Lecina, E. Playán, A model for the simulation of water flows in irrigation districts II: application, ASCE Journal of Irrigation and Drainage Engineering 132 (4) (2006) 322–331.

[16] G. Lorenzini, Simplified modelling of sprinkler droplet dynamics, Biosystems Engineering 87 (1) (2004) 1–11.

[17] A. Martínez-Cob, J. M. Faci, A. Bercero, Evapotranspiración y necesidades de riego de los principales cultivos en las comarcas de Aragón, Institución Fernando el Católico, Zaragoza (1998).

[18] J. L. Merriam, J. Keller, Farm irrigation system evaluation: a guide for management, Utah State University, Logan, Utah, 1978.

[19] J. Montero, J. M. Tarjuelo, P. Carrión, SIRIAS: a simulation model for sprinkler irrigation II: calibration and validation of the model, Irrigation Science 20 (2001) 73–84.

[20] J. Montero, J. M. Tarjuelo, P. Carrión, Sprinkler droplet size distribution measured with an optical spectropluviometer, Irrigation Science 22 (2) (2003) 47–56.

[21] J. E. Naranjo, Los efectos esperados del plan nacional de regadíos, Agricultura 842 (2002) 557–562.

[22] E. Playán, R. Salvador, J. M. Faci, N. Zapata, A. Martínez-Cob, I. Sánchez, Day and night wind drift and evaporation losses in sprinkler solid-sets and moving laterals, Agricultural Water Management 76 (3) (2005) 139–159.

[23] E. Playán, N. Zapata, J. M. Faci, D. Tolosa, J. L. Lacueva, J. Pelegrín, R. Salvador, I. Sánchez, A. Lafita, Assessing sprinkler irrigation uniformity using a ballistic simulation model, Agricultural Water Management 84 (1–2) (2006) 89–100.

[24] R. Salvador, Estudio de las pérdidas por evaporación y arrastre en los sistemas de riego por aspersión. diferencias entre riegos diurnos y nocturnos, Proyecto fin de carrera, Universitat de Lleida, Lleida (2003).

[25] R. Salvador, E. Playán, C. Bautista-Capetillo, J. Burguete, N. Zapata, A. Serreta, A photographic method for drop characterization in agricultural sprinklers, ASCE Journal of Irrigation and Drainage Engineering submitted.

[26] I. Seginer, D. Nir, R. D. von Bernuth, Simulation of wind-distorted sprinkler patterns, ASCE Journal of Irrigation and Drainage Engineering 117 (2) (1991) 285–306.

[27] J. M. Tarjuelo, El riego por aspersión y su tecnología, Mundiprensa, Madrid, 1995.

[28] J. M. Tarjuelo, P. Carrión, M. Vicente, Simulación de la distribución del riego por aspersión en condiciones de viento, Investigación Agraria. Producción y Protección Vegetal 9 (2) (1994) 255–271.

[29] N. Zapata, E. Playán, A. Skhiri, J. Burguete, A collective solid-set sprinkler irrigation controller for optimum water productivity, ASCE Journal of Irrigation and Drainage Engineering In press.